

Kinetics and Mechanism of the Oxidation of Alkylaromatic Compounds by a *trans*-Dioxoruthenium(VI) ComplexWilliam W. Y. Lam,[†] Shek-Man Yiu,[†] Douglas T. Y. Yiu,[†] Tai-Chu Lau,^{*,†} Wing-Ping Yip,[‡] and Chi-Ming Che^{*,†}

Department of Biology and Chemistry, City University of Hong Kong, Tat Chee Avenue, Kowloon Tong, Hong Kong, China, and Department of Chemistry and Open Laboratory of the Institute of Molecular Technology for Drug Discovery and Synthesis, The University of Hong Kong, Pokfulam Road, Hong Kong, China.

Received July 8, 2003; Revised Manuscript Received September 10, 2003

The oxidations of a series of 21 alkylaromatic compounds by *trans*-[Ru^{VI}(L)(O)₂]²⁺ (L = 1,12-dimethyl-3,4:9,10-dibenzo-1,12-diaza-5,8-dioxacyclopentadecane) have been studied in CH₃CN. Toluene is oxidized to benzaldehyde and a small amount of benzyl alcohol. 9,10-Dihydroanthracene is oxidized to anthracene and anthraquinone. Other substrates give oxygenated products. The kinetics of the reactions were monitored by UV–vis spectrophotometry, and the rate law is: $-d[\text{Ru}^{\text{VI}}]/dt = k_2[\text{Ru}^{\text{VI}}][\text{ArCH}_3]$. The kinetic isotope effects for the oxidation of toluene/*d*₈-toluene and fluorene/*d*₁₀-fluorene are 15 and 10.5, respectively. A plot of ΔH^\ddagger versus ΔS^\ddagger is linear, suggesting a common mechanism for all the substrates. In the oxidation of para-substituted toluenes, a linear correlation between $\log k_2$ and σ^0 values is observed, consistent with a benzyl radical intermediate. A linear correlation between ΔG^\ddagger and ΔH^\ddagger (the difference between the strength of the bond being broken and that being formed in a H-atom transfer step) is also found, which strongly supports a hydrogen atom transfer mechanism for the oxidation of these substrates by *trans*-[Ru^{VI}(L)(O)₂]²⁺. The slope of (0.61 ± 0.06) is in reasonable agreement with the theoretical slope of 0.5 predicted by Marcus theory.

Introduction

The oxidation of hydrocarbons by metal-oxo species has received much attention in recent years because of its fundamental interest and its relevance to a number of industrial and biological processes.^{1–5} A number of mechanisms are apparently operating, depending on the nature of

the metal oxo species, the substrates and the solvents. The oxidation of toluene by MnO₄[−] proceeds through a hydrogen atom transfer mechanism in nonpolar solvents but a hydride transfer mechanism in aqueous solutions.² The oxidation of toluene by CrO₂Cl₂ in cyclohexane solution also occurs by hydrogen atom transfer.³ On the other hand, the oxidation of alkylbenzenes by a ruthenium(IV) oxo species, [Ru(tpy)-(bpy)O]²⁺ (tpy = 2,2':6',2''-terpyridine, bpy = 2,2'-bipyridine) proceeds by a hydride transfer mechanism both in water and in CH₃CN.⁴ The oxidation of alkylaromatic hydrocarbons by manganese oxo dimers may occur by hydrogen atom transfer, electron transfer, or hydride transfer, depending on the oxidation states of the manganese and on the substrate.⁵

We report here results of a kinetic and mechanistic study of the oxidation of a variety of alkylaromatic compounds in CH₃CN by a cationic *trans*-dioxoruthenium(VI) complex, *trans*-[Ru^{VI}(L)(O)₂]²⁺, where L = 1,12-dimethyl-3,4:9,10-

* Corresponding authors. E-mail: bhtclau@cityu.edu.hk; cmche@hku.hk.

[†] City University of Hong Kong.

[‡] The University of Hong Kong.

- (1) (a) *Biomimetic Oxidations Catalyzed by Transition Metal Complexes*; Meunier, B., Ed.; Imperial College Press: London, 2000. (b) *Metal-Oxo and Metal-Peroxo Species in Catalytic Oxidations*; Meunier, B., Ed.; Springer: Berlin, 2000. (c) Weissermel, K.; Arpe, H.-J. *Industrial Organic Chemistry*; VCH: New York, 1997. (d) Davies, J. A.; Watson, P. L.; Greenberg, A.; Liebman, J. F. *Selective Hydrocarbon Activation: Principles and Progress*. VCH: New York, 1990. (e) Kochi, J. K.; Sheldon, R. A. *Metal-Catalyzed Oxidations of Organic Compounds*. Academic Press: New York, 1981.
- (2) (a) Gardner, K. A.; Mayer, J. M. *Science* **1995**, *269*, 1849–1851. (b) Gardner, K. A.; Kuehnert, L. L.; Mayer, J. M. *Inorg. Chem.* **1997**, *36*, 2069–2078. (c) Mayer, J. M. *Acc. Chem. Res.* **1998**, *31*, 441–450.
- (3) Cook, G. K.; Mayer, J. M. *J. Am. Chem. Soc.* **1995**, *117*, 7139–7156.
- (4) Thompson, M. S.; Meyer, T. J. *J. Am. Chem. Soc.* **1982**, *104*, 5070–5076.

- (5) (a) Wang, K.; Mayer, J. M. *J. Am. Chem. Soc.* **1997**, *119*, 1470–1471. (b) Lockwood, M. A.; Wang, K.; Mayer, J. M. *J. Am. Chem. Soc.* **1999**, *121*, 11894–11895. (c) Larson, A. S.; Wang, K.; Lockwood, M. A.; Rice, G. L.; Won, T.-J.; Lovell, S.; Sadilek, M.; Tureček, F.; Mayer, J. M. *J. Am. Chem. Soc.* **2002**, *124*, 10112–10123.

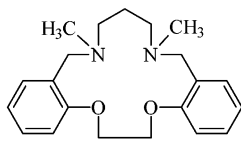


Figure 1. Structure of L.

dibenzo-1,12-diaza-5,8-dioxacyclopentadecane (Figure 1).⁶ There are quite a number of stable, *trans*-dioxoruthenium-(VI) complexes containing macrocyclic tertiary amine or polypyridyl ligands.⁷ These complexes are, in general, potent oxidants for a variety of organic and inorganic substrates. They often react via different mechanisms from that of ruthenium(IV) monooxo species such as $[\text{Ru}(\text{tpy})(\text{bpy})\text{O}]^{2+}$ and related species. For example, in the oxidation of phenol by $[\text{Ru}^{\text{IV}}(\text{bpy})_2(\text{py})(\text{O})]^{2+}$, a mechanism that involves electrophilic attack on the aromatic ring was proposed.⁸ On the other hand, the oxidation of phenol by *trans*- $[\text{Ru}^{\text{VI}}(\text{L})(\text{O})_2]^{2+}$ occurs by hydrogen atom transfer.⁹ The kinetics of the oxidation of toluene, cumene, and ethylbenzene by *trans*- $[\text{Ru}^{\text{VI}}(\text{L})(\text{O})_2]^{2+}$ have been reported, and on the basis of a large kinetic isotope effect for the oxidation of ethylbenzene ($k_{\text{C}_8\text{H}_{10}}/k_{\text{C}_8\text{D}_{10}} = 16$), a hydrogen atom transfer mechanism was proposed.¹⁰ However, large deuterium isotope effects are also consistent with electron transfer¹¹ and hydride transfer mechanisms^{5c} for oxidative C–H bond activation. To provide further insights into the reaction mechanism, we have studied a series of 21 alkylaromatic compounds with a wide range of oxidation potentials and α C–H bond dissociation energies. The effects of substituents, nucleophiles, and bases on the reaction rates as well as the correlation of rate constants with oxidation potentials and α C–H bond dissociation energies of the substrates have been investigated. We were also interested to see if there is a change of reaction mechanism along the series, since for electron-rich substrates an electron transfer pathway may become favorable. *trans*- $[\text{Ru}^{\text{VI}}(\text{L})(\text{O})_2]^{2+}$ is a reasonably good one-electron oxidant, E^0 for the *trans*- $[\text{Ru}^{\text{VI}}(\text{L})(\text{O})_2]^{2+}/\text{trans}$ - $[\text{Ru}^{\text{V}}(\text{L})(\text{O})_2]^+$ couple is 0.94 V vs NHE,⁶ and the self-exchange rate is $1 \times 10^5 \text{ M}^{-1} \text{ s}^{-1}$ at 25.0 °C.⁹

Experimental Section

Materials. *trans*- $[\text{Ru}^{\text{VI}}(\text{L})(\text{O})_2](\text{PF}_6)_2$ was prepared by a literature procedure.⁶ Aromatic compounds were purified before use.¹² Toluene (RDH) was washed with cold concentrated H_2SO_4 ,

followed by distilled water, and then 5% aqueous NaHCO_3 . It was dried with CaSO_4 and then passed through a column of neutral alumina. Ethylbenzene (Aldrich 99%) and cumene (Merck 99%) were purified by similar procedures. Mesitylene was chromatographed on silica gel and then distilled from sodium. Durene (1,2,4,5-tetramethylbenzene) (Aldrich 98%) was chromatographed on neutral alumina and then recrystallized from aqueous ethanol. Isodurene (1,2,3,5-tetramethylbenzene), 1,2,3,4-tetramethylbenzene, 1,2,4-trimethylbenzene, and 1,2,3-trimethylbenzene were passed through a column of neutral alumina, then refluxed over sodium, and finally distilled under reduced pressure. Pentamethylbenzene (Aldrich 99%) was successively recrystallized from absolute ethanol, toluene, and methanol. Hexamethylbenzene (Aldrich 99%), diphenylmethane (Aldrich 99%), triphenylmethane (Aldrich 99%), 9,10-dihydroanthracene (DHA) (Aldrich 97%), and xanthene (Aldrich 99%) were recrystallized from ethanol. Fluorene (Aldrich 98%) was purified by chromatography of a petroleum ether (bp 40–60 °C) solution on neutral alumina with benzene as eluent, followed by recrystallization from 95% ethanol, 90% acetic acid, and then again from ethanol. 4-Tolunitrile (Aldrich 98%) was crystallized from petroleum ether. Anthracene (Merck) was recrystallized from cyclohexane and then chromatographed on alumina with *n*-hexane as eluent. It was then recrystallized twice from cyclohexane. Anthraquinone (Aldrich) was recrystallized from benzene and then washed with absolute ethanol. 2-Bromotoluene (Acrös), 2,5-dibromotoluene (Acrös), 2,6-dimethoxytoluene (Acrös), 4-methylanisole (Acrös 99%), 4-chlorotoluene (Aldrich 98%), *p*-xylene (Aldrich 99+% anhydrous), d_8 -toluene (Aldrich), and d_{10} -fluorene (Aldrich) were used as received. Acetonitrile (AR grade) was refluxed overnight with KMnO_4 and then distilled over CaH_2 under argon.

Kinetics. The kinetics of the reaction were studied by using either a Hewlett-Packard 8452A UV–vis spectrophotometer or a Hi-Tech Scientific SF-61 stopped-flow spectrophotometer. The concentrations of the alkylaromatic compounds (2×10^{-3} to 1 M) were at least in 10-fold excess as that of Ru^{VI} (5×10^{-5} to 1×10^{-4} M). The reaction progress was monitored by observing absorbance changes at 400 nm (λ_{max} of Ru^{VI}). Pseudo-first-order rate constants, k_{obs} , were obtained by nonlinear least-squares fits of A_t vs time t according to the equation $A_t = A_{\infty} + (A_0 - A_{\infty}) \exp(-k_{\text{obs}}t)$, where A_0 and A_{∞} are the initial and final absorbances, respectively. Kinetics carried out in the air and under argon were found to give the same rate constants; therefore, most kinetic studies were done in the air.

Product Analysis. The organic products were determined by a Hewlett-Packard 6890 gas chromatograph equipped with DB-5MS and FFAP capillary columns. GC–MS measurements were carried out on a HP 5890 gas chromatograph interfaced to a HP5970 mass selective detector.

The analysis of products resulting from the oxidation of toluene was typically carried out as follows. Ru^{VI} (3 mg, 3.9×10^{-3} mmol) was added to a mixture containing 0.42 mL (3.9 mmol) of toluene and 0.5 mL of CH_3CN at room temperature in the dark with vigorous stirring. Analysis by GC and GC–MS after 10 h using chlorobenzene as internal standard indicated that $\sim 1.3 \times 10^{-3}$ mmol of benzaldehyde and $\sim 1.7 \times 10^{-4}$ mmol of benzyl alcohol were produced. This corresponds to yields of 66 and 4%, respectively, for benzaldehyde and benzyl alcohol, since *trans*- $[\text{Ru}^{\text{VI}}(\text{L})(\text{O})_2]^{2+}$ functions as a two-electron oxidant. No benzoic acid and no diphenylmethane products were detected.

In radical trap experiments for toluene oxidation, the experimental conditions were the same as above except that 39 μL (3.9×10^{-1} mmol) of BrCCl_3 was also added. The yields of benzaldehyde and

- (6) Che, C. M.; Tang, W. T.; Wong, W. T.; Lai, T. F. *J. Am. Chem. Soc.* **1989**, *111*, 9048–9056.
 (7) (a) Che, C. M.; Yam, V. W. *Adv. Inorg. Chem.* **1992**, *39*, 233–325. (b) Che, C. M.; Tang, W. T.; Lee, W. O.; Wong, K. Y.; Lau, T. C. *J. Chem. Soc., Dalton Trans.* **1992**, 1551–1556.
 (8) Seok, W. K.; Meyer, T. J. *J. Am. Chem. Soc.* **1988**, *110*, 7358–7367.
 (9) Yiu, D. T. Y.; Lee, M. F. W.; Lam, W. W. Y.; Lau, T. C. *Inorg. Chem.* **2003**, *42*, 1225–1232.
 (10) Che, C. M.; Tang, W. T.; Wong, K. Y.; Li, C. K. *J. Chem. Soc., Dalton Trans.* **1991**, 3277–3280.
 (11) (a) Schlessener, C. J.; Amatore, C.; Kochi, J. K. *J. Am. Chem. Soc.* **1984**, *106*, 3567–3577. (b) Bockman, T. M.; Hubig, S. M.; Kochi, J. K. *J. Am. Chem. Soc.* **1998**, *120*, 2826–2830.
 (12) Armarego, W. L. F.; Perrin, D. D. *Purification of Laboratory Chemicals*, 4th ed.; Reed Educational and Professional Publishing Ltd.: Oxford, 1996.

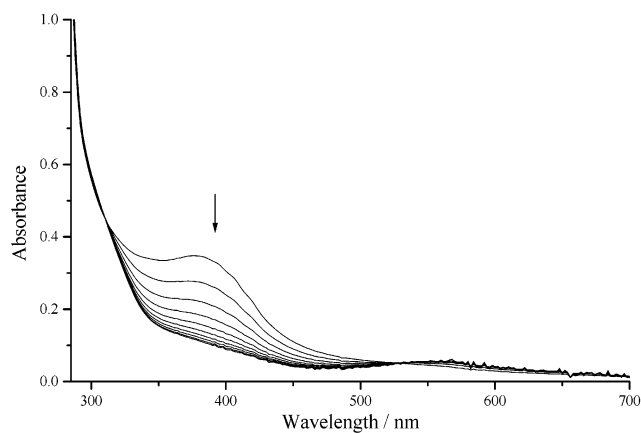


Figure 2. Spectral changes at 540-s intervals during the oxidation of hexamethylbenzene (8×10^{-3} M) by $trans\text{-}[\text{Ru}^{\text{VI}}(\text{L})(\text{O})_2]^{2+}$ (2×10^{-4} M) at 298 K in CH_3CN .

benzyl alcohol were 65 and 4%, respectively, which are the same as in the absence of BrCCl_3 . No benzyl bromide was detected.

The kinetic isotope effects (KIE) for toluene oxidation were studied using an equimolar mixture of toluene and d_8 -toluene (0.21 mL each). The products were analyzed by GC using a FFAP column and by GC-MS using a DB-5MS column. The KIE ($k_{\text{H}}/k_{\text{D}} = 15 \pm 1$) was obtained by taking the ratio of the areas of the products.

The analysis of products resulting from the oxidation of 9,10-dihydroanthracene was typically carried out as follows. Ru^{VI} (2 mg, 2.7×10^{-3} mmol) was added to a mixture containing 22 mg (0.12 mmol) of DHA and 1.0 mL of CH_3CN at room temperature in the dark with vigorous stirring. After 10 min, analysis by GC and ^1H NMR (CDCl_3) indicated the formation of anthracene (1.7×10^{-3} mmol, 63%) and anthraquinone (2.2×10^{-4} mmol, 33%). Anthracene was also determined by UV-vis spectrophotometry ($\epsilon = 7475 \text{ M}^{-1} \text{ cm}^{-1}$ at 358 nm) with similar results.

Results

Spectral Changes and Products. The UV-vis spectral changes that occurred when $trans\text{-}[\text{Ru}^{\text{VI}}(\text{L})(\text{O})_2]^{2+}$ was mixed with an excess of hexamethylbenzene in CH_3CN at 25 °C is shown in Figure 2. The spectral changes for the oxidation of other alkylaromatic compounds were similar. In all cases, the final spectrum was consistent with quantitative formation of $trans\text{-}[\text{Ru}^{\text{IV}}(\text{L})(\text{O})(\text{CH}_3\text{CN})]^{2+}$.⁶ Subsequent reduction of $trans\text{-}[\text{Ru}^{\text{IV}}(\text{L})(\text{O})(\text{CH}_3\text{CN})]^{2+}$ to $trans\text{-}[\text{Ru}^{\text{II}}(\text{L})(\text{CH}_3\text{CN})_2]^{2+}$ was not observed for at least 24 h. No charge-transfer (CT) complexes between $trans\text{-}[\text{Ru}^{\text{VI}}(\text{L})(\text{O})_2]^{2+}$ and the substrates were observed under our experimental conditions, where the concentrations of Ru^{VI} ranged from 5×10^{-5} to 1×10^{-4} M, and that of the aromatics ranged from 2×10^{-3} to 1 M. CT complexes have been observed with aromatic hydrocarbons and MnO_4^- ,^{2b} CrO_2Cl_2 ,³ and OsO_4 .¹³

The oxidation of toluene results in the formation of 66% benzaldehyde and 4% benzyl alcohol, as determined by GC and GC-MS. The yields are based on $trans\text{-}[\text{Ru}^{\text{VI}}(\text{L})(\text{O})_2]^{2+}$ acting as a two-electron oxidant. No other products, such as benzoic acid and diphenylmethanes, were detected. The yields were unaffected by the presence of BrCCl_3 or O_2 . In the oxidation of DHA, the two-electron oxidized product

anthracene (63%) and the eight-electron oxidized product anthraquinone (33%) were observed. The oxidation of ethylbenzene to acetophenone (61%) and 1-phenylethanol (37%) and of cumene to 2-phenyl-2-propanol (70%) have previously been reported.⁶ Yields of less than 100% were also observed in the oxidation of toluene by CrO_2Cl_2 ³ and of various alkylaromatic compounds by ${}^n\text{Bu}_4\text{N}[\text{MnO}_4]$.^{2b} Attempts to identify more products by HPLC were unsuccessful.

Kinetics. The kinetics of the oxidation of alkylaromatic compounds by $trans\text{-}[\text{Ru}^{\text{VI}}(\text{L})(\text{O})_2]^{2+}$ were monitored by observing absorbance changes at 400 nm (λ_{max} of Ru^{VI}). In the presence of at least a 10-fold excess of aromatics, clean pseudo-first-order kinetics were observed for over three half-lives. No induction periods were observed for any of the substrates. The pseudo-first-order rate constant, k_{obs} , was independent of the concentration of the Ru^{VI} complex but depended linearly on the concentration of the hydrocarbon. Thus, the experimentally determined rate law is as shown in eq 1.

$$\frac{d[\text{Ru}^{\text{VI}}]}{dt} = k_2[\text{Ru}^{\text{VI}}][\text{ArCH}_3] = k_{\text{obs}}[\text{Ru}^{\text{VI}}] \quad (1)$$

In the oxidation of DHA and toluene, the rate constants are unaffected by the presence of H_2O (1%), pyridine (1 mM), and salt (${}^n\text{Bu}_4\text{N}[\text{PF}_6]$, 2 mM). The rate constants are also the same in the air or under argon. Kinetic data are collected in Table 1, the second-order rate constants are listed as k'_2 , which is equal to k_2 divided by the number of reactive hydrogen atoms in each substrate. For example, the number of reactive hydrogens for toluene, ethylbenzene, isopropylbenzene, and hexamethylbenzene are 3, 2, 1, and 18, respectively. The activation parameters ΔH^\ddagger and ΔS^\ddagger were determined by studying the kinetics over a 30–40 °C temperature range; they are also listed on a per reactive hydrogen basis in Table 1.

Kinetic Isotope Effects (KIE). The KIE for the oxidation of toluene was determined by both the kinetics method and product analysis. The values obtained for the two methods are in excellent agreement: $k_{\text{C}_7\text{H}_8}/k_{\text{C}_7\text{D}_8} = 14.3 \pm 0.5$ (kinetics) and 15 ± 1 (product analysis). In the oxidation of fluorene and d_{10} -fluorene the KIE was found to be 10.5 ± 0.5 using the kinetics method. A KIE of 16 has also been previously reported for the oxidation of ethylbenzene and d_{10} -ethylbenzene using the kinetics method.¹⁰

Discussion

Overview of the Reactions. In the presence of excess hydrocarbon, $trans\text{-}[\text{Ru}^{\text{VI}}(\text{L})(\text{O})_2]^{2+}$ is reduced to $trans\text{-}[\text{Ru}^{\text{IV}}(\text{L})(\text{O})(\text{CH}_3\text{CN})]^{2+}$ in CH_3CN . No intermediate Ru^{V} species was observed, as in the reaction of $trans\text{-}[\text{Ru}^{\text{VI}}(\text{L})(\text{O})_2]^{2+}$ with a number of other reducing agents.^{9–10,14–16} The

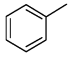
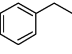
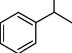
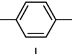
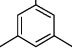
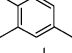
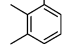
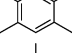
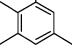
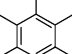
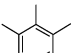
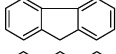
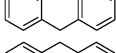
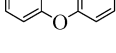
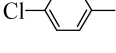
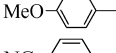
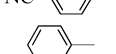
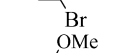
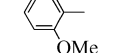
(13) Wallis, J. M.; Kochi, J. K. *J. Am. Chem. Soc.* **1988**, *110*, 8207–8223.

(14) Che, C. M.; Tang, W. T.; Lee, W. O.; Wong, K. Y.; Lau, T. C. *J. Chem. Soc., Dalton Trans.* **1992**, 1551–1556.

(15) Che, C. M.; Li, C. K.; Tang, W. T.; Yu, W. Y. *J. Chem. Soc., Dalton Trans.* **1992**, 3153–3158.

(16) Yiu, D. T. Y.; Chow, K. H.; Lau, T. C. *J. Chem. Soc., Dalton Trans.* **2000**, 17–20.

Table 1. Second-Order Rate Constants at 298.0 K and Activation Parameters for the Oxidation of Alkylaromatic Compounds by *trans*-[Ru^{VI}(L)(O)₂]²⁺

No.	Substrate	$k_2'/M^{-1}s^{-1}{}^a$	$\Delta H^\ddagger{}^b$ (kcal mol ⁻¹)	$\Delta S^\ddagger{}^b$ (cal K ⁻¹ mol ⁻¹)	BDE ^c (kcal mol ⁻¹)	$E^0{}^d$ [V(NHE)]
1		(3.70 ± 0.13) × 10 ⁻⁵ (6.63 ± 0.07) × 10 ⁻⁵ ^e	34.1 ± 1.4	36 ± 5	89.8	2.64
2		(1.82 ± 0.05) × 10 ⁻³	25.7 ± 0.6	15 ± 2	85.4	2.62
3		(5.38 ± 0.03) × 10 ⁻³	24.7 ± 0.8	14 ± 2	84.4	2.53
4		(1.62 ± 0.03) × 10 ⁻⁴	27.1 ± 1.9	15 ± 3		2.30
5		(2.19 ± 0.01) × 10 ⁻⁴	27.8 ± 0.7	18 ± 2		2.35
6		(3.01 ± 0.07) × 10 ⁻⁴	27.1 ± 1.0	16 ± 3		2.13
7		(2.19 ± 0.02) × 10 ⁻⁴	27.9 ± 0.7	19 ± 2		2.23
8		(6.29 ± 0.19) × 10 ⁻⁴	21.2 ± 1.5	-(2 ± 2)		1.94
9		(5.56 ± 0.03) × 10 ⁻⁴	21.7 ± 1.0	-(1 ± 2)		1.95
10		(1.13 ± 0.07) × 10 ⁻³	18.3 ± 0.9	-(11 ± 2)		1.87
11		(3.75 ± 0.04) × 10 ⁻³	16.6 ± 0.3	-(14 ± 2)		1.74
12	Ph ₂ CH ₂	(1.03 ± 0.03) × 10 ⁻²	18.0 ± 1.3	-(7 ± 2)	82.0	
13	Ph ₃ CH	(6.20 ± 0.06) × 10 ⁻²	16.7 ± 1.2	-(8 ± 2)	81.0	
14		1.58 ± 0.03	13.8 ± 0.5	-(11 ± 2)	80.1	1.91
15		7.45 ± 0.15	9.0 ± 1.2	-(24 ± 3)	78.0	1.94
16		49.7 ± 0.4	5.7 ± 0.9	-(32 ± 3)	75.5	
17		(1.62 ± 0.07) × 10 ⁻³ ^e				
18		(2.89 ± 0.03) × 10 ⁻³ ^e				
19		(1.17 ± 0.03) × 10 ⁻² ^e				
20		(2.29 ± 0.04) × 10 ⁻⁵ ^e				
21		(8.27 ± 0.11) × 10 ⁻⁶ ^e				

^a Values are at 298 K and corrected per active hydrogen of the substrates. ^b Temperature range 288–328 K. ^c Data are from ref 32. ^d Data are from ref 23. ^e Value at 313.0 K and corrected per active hydrogen of the substrate.

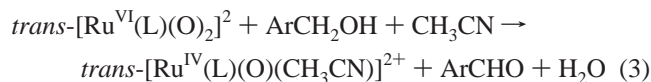
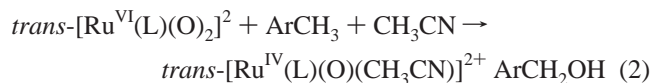
failure to detect a Ru^V intermediate can be due to a number of possibilities. If the reaction involves H⁻ transfer, as in the oxidation of alcohols¹⁴ and phosphite,¹⁶ the intermediate would be *trans*-[Ru^{IV}(L)(O)(OH)]⁺. In the oxidation of excess [Ru^{II}(NH₃)₄(isn)₂]²⁺ (isn = isonicotinamide) in aqueous acidic solution, *trans*-[Ru^V(L)(O)₂]⁺ is first produced, which is then protonated to give *trans*-[Ru^V(L)(O)(OH)]²⁺.¹⁷

trans-[Ru^V(L)(O)(OH)]²⁺ is a stronger oxidant than [Ru^{VI}(L)(O)₂]²⁺, it is more rapidly reduced by excess [Ru^{II}(NH₃)₄(isn)₂]²⁺, and hence, no intermediate Ru^V is observed.⁶ In the absence of excess reducing agents, Ru^V may still not be observed because it undergoes rapid acid-catalyzed dispro-

(17) Li, C. K. Ph.D. Thesis, University of Hong Kong, China, 1991.

portionation.^{6,17,18} The oxidation of phenols involves H[•] transfer to produce *trans*-[Ru^V(L)(O)(OH)]²⁺, which again is more rapidly reduced by phenoxy radical or excess phenol.

The major reaction pathways occurring in the oxidation of alkylaromatic compounds with primary or secondary C–H bonds by *trans*-[Ru^{VI}(L)(O)₂]²⁺ can be represented by eqs 2 and 3:



The initial product is the alcohol, which is then further oxidized to the corresponding aldehyde or ketone. The carbonyl compound is the major product because, in general, alcohols are oxidized much more rapidly than hydrocarbons by *trans*-[Ru^{VI}(L)(O)₂]²⁺, i.e., reaction 3 occurs much more rapidly than reaction 2.⁷ The mechanism for the oxidation of alcohols by *trans*-dioxoruthenium(VI) complexes has been investigated.⁷ In the oxidation of alkylaromatic hydrocarbons with tertiary C–H bonds, such as cumene, the major product is the corresponding alcohol. In the case of DHA, the major product is anthracene. Independent experiments showed that anthracene is more slowly oxidized than DHA.

The second-order rate constants span more than 6 orders of magnitude (Table 1). Toluene has the highest α C–H bond dissociation energy and is one of the least reactive substrates (BDE = 89.8 kcal mol⁻¹, *k*₂ = 1.11 × 10⁻⁴ M⁻¹ s⁻¹ at 25.0 °C), while xanthene has the lowest α C–H bond dissociation energy and is the most reactive substrate (BDE = 75.5 kcal mol⁻¹, *k*₂ = 9.94 × 10¹ M⁻¹ s⁻¹ at 25.0 °C). The rate constant for the oxidation of toluene by *trans*-[Ru^{VI}(L)(O)₂]²⁺ is similar to that by Cr₂O₂Cl₂ (*k*₂ = 1.9 × 10⁻⁴ M⁻¹ s⁻¹ at 29.4 °C)³ but is much faster than that by ⁿBu₄N[MnO₄] (*k*₂ = 1.4 × 10⁻⁷ M⁻¹ s⁻¹ at 25.0 °C).^{2b}

Correlation between Δ*H*[‡] and Δ*S*[‡]. Compensation Effects. Both Δ*H*[‡] and Δ*S*[‡] vary along the series of alkylaromatic compounds, and a compensating effect is observed, i.e., when Δ*H*[‡] increases, Δ*S*[‡] does so as well.^{19,20} A plot of Δ*H*[‡] versus Δ*S*[‡] is linear (Figure 3), suggesting that all the hydrocarbons react by a common mechanism. The observation of compensation effect may be interpreted as follows. For substrates with stronger C–H bonds (larger Δ*H*[‡]), a weaker attraction between Ru=O and C–H occurs in the transition state, and this will lead to a less ordered state (larger Δ*S*[‡]). This compensating effect appears to be rather large; Δ*H*[‡] ranges from 5.7 to 34 kcal mol⁻¹, while Δ*S*[‡] ranges from -24 to 36 cal K⁻¹ mol⁻¹. Notably toluene has a rather positive Δ*S*[‡] value of 36 cal K⁻¹ mol⁻¹, while negative Δ*S*[‡] values are found for the oxidation of toluene by other metal-oxo species such as ⁿBu₄N[MnO₄],^{2b} CrO₂-

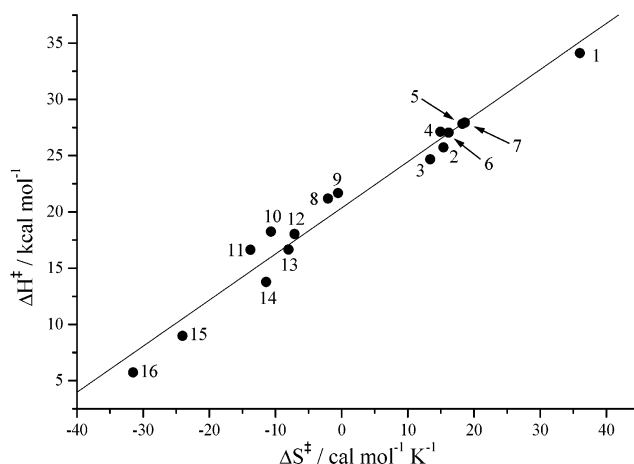
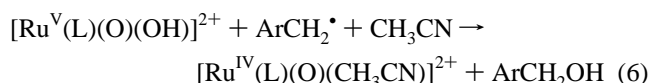
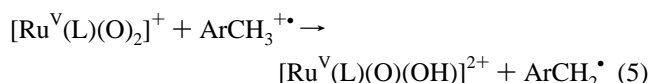
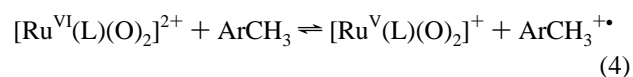


Figure 3. Plot of Δ*H*[‡] versus Δ*S*[‡] for the oxidation of alkylaromatic compounds by [Ru^{VI}(L)(O)₂]²⁺ in CH₃CN (slope = 0.41 ± 0.02, *r* = 0.984).

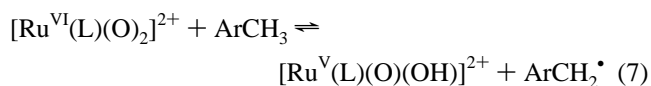
Cl₂,³ and [(phen)₂Mn^{IV}(μ-O)₂Mn^{III}(phen)₂]³⁺.^{5c} A correlation between Δ*H*[‡] and Δ*S*[‡] has also been found for the oxidation of hydrocarbons by CrO₂Cl₂.³

Mechanisms of C–H Bond Activation. The observation of a correlation between Δ*H*[‡] and Δ*S*[‡] together with other evidence presented below suggests a common mechanism for the oxidation of the alkylaromatic compounds. There are three possible mechanisms for the oxidation of the α-CH bonds (eq 2) in these hydrocarbons.

Outer-sphere electron transfer:

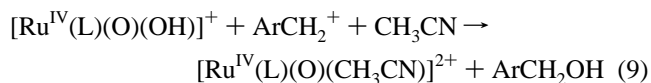
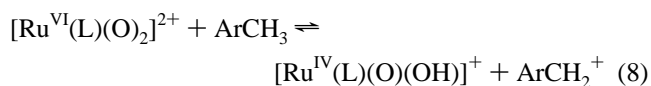


Hydrogen atom transfer:



Subsequent reaction occurs as in eq 6.

Hydride transfer:



Although large H/D kinetic isotope effects are observed, they cannot be taken as a conclusive evidence for any of the above mechanisms since all three pathways can have large KIE. In an outer-sphere electron transfer mechanism, a larger KIE can result if proton transfer from ArCH₃⁺ is rate-limiting (eq 5 in this case).¹¹ We present other evidence below that supports a hydrogen atom transfer mechanism

(18) Che, C. M.; Lau, K.; Lau, T. C.; Poon, C. K. *J. Am. Chem. Soc.* **1990**, *112*, 5176–5181.

(19) Liu, L.; Guo, Q.-X. *Chem. Rev.* **2001**, *101*, 673–685.

(20) Espenson, J. H. *Chemical Kinetics and Reaction Mechanisms*, 2nd ed.; McGraw-Hill: New York, 1995; pp 164–165.

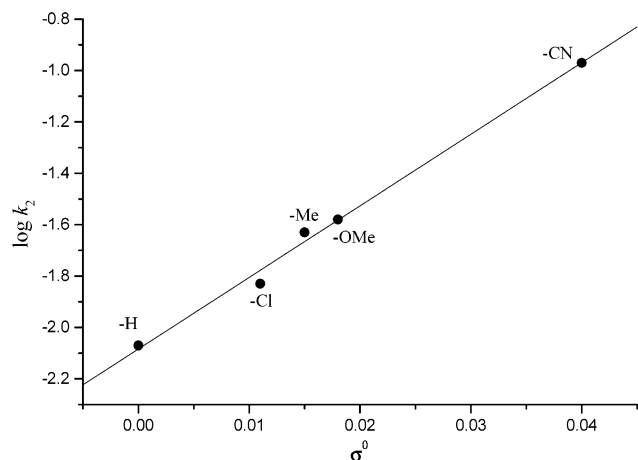


Figure 4. Hammett plot of $\log k_2$ versus σ^0 for the oxidation of para-substituted toluenes by $\text{trans-}[\text{Ru}^{\text{VI}}(\text{L})(\text{O})_2]^{2+}$ in CH_3CN at 313 K (slope = 27.9 ± 1.3 , $r = 0.997$).

for the oxidation of these alkylaromatic compounds by $[\text{Ru}^{\text{VI}}(\text{L})(\text{O})_2]^{2+}$.

Substituent Effects. Hammett Correlation. The electronic effects of a substituent in the para position of toluene on the rate constants have been investigated at 313 K (Table 1). Both electron-donating and electron-withdrawing substituents are found to cause an increase in rate constants; hence, there is no correlation with either Hammett σ or σ^+ values. A similar observation is reported for oxidation by ${}^n\text{Bu}_4\text{N}[\text{MnO}_4]$.^{2b} However, there is a good correlation with σ^0 values (Figure 4),²¹ which is consistent with a benzyl radical intermediate produced by hydrogen atom transfer. A benzyl radical intermediate can be stabilized by both electron-withdrawing and electron-donating substituents.²¹ On the other hand, a benzyl cation intermediate, produced by hydride transfer, would be stabilized by electron-donating substituents but destabilized by electron-withdrawing substituents. Moreover, 4-methylanisole and *p*-xylene react only 3 times faster than toluene. If the H^- transfer mechanism operates, they should be more reactive. Product analysis also did not reveal any evidence for a hydride transfer mechanism; no diaryl-methane products were detected in the oxidation of toluene by $\text{trans-}[\text{Ru}^{\text{VI}}(\text{L})(\text{O})_2]^{2+}$. In the oxidation of toluene by $[(\text{phen})_2\text{Mn}^{\text{IV}}(\mu\text{-O})_2\text{Mn}^{\text{III}}(\text{phen})_2]^{3+}$, tolyl-phenylmethane products were detected, which was interpreted as a result of hydride abstraction to produce benzyl cation that alkylates the excess toluene present.^{5c}

Significant steric effects are observed when bulky groups are present in the ortho positions of toluene. For example, 2-bromotoluene and 2,6-dimethoxytoluene are less reactive than toluene by 40 and 110 times, respectively. This is consistent with a mechanism involving attack of $\text{Ru}=\text{O}$ on an α C–H bond of the substrate and is not consistent with an electron transfer mechanism. Similar steric effects have also been observed in hydrogen atom abstraction from phenols by $\text{trans-}[\text{Ru}^{\text{VI}}(\text{L})(\text{O})_2]^{2+}$.⁹

Effects of Added Nucleophiles and Bases. In the oxidation of DHA and toluene in CH_3CN , the rate constants are

(21) Wayner, D. D. M.; Arnold, D. R. *Can. J. Chem.* **1985**, *63*, 2378–2383.

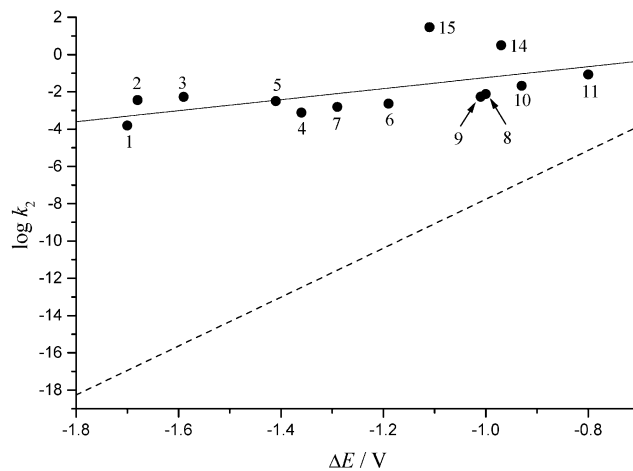


Figure 5. Plot of $\log k_2$ versus $\Delta E^0 (E^0(\text{Ru}^{\text{VI}}/\text{Ru}^{\text{V}} - E^0(\text{ArCH}_3^+/\text{ArCH}_3))$ for the oxidation of ArCH_3 by $\text{trans-}[\text{Ru}^{\text{VI}}(\text{L})(\text{O})_2]^{2+}$ in CH_3CN at 298.0 K (slope = 2.9 ± 1.1 , $r = 0.62$). The dotted line represents the theoretical line calculated according to eq 10.

unaffected by the presence of H_2O (1%) and pyridine (1 mM). H_2O is known to accelerate the oxidation of isopropylbenzene by $[\text{Ru}(\text{bpy})_2(\text{py})(\text{O})]^{2+}$ in CH_3CN ; it was proposed that the function of H_2O was to assist in the loss of hydride ions from the substrates.⁴ In the oxidation of methylarenes by $[\text{Fe}(\text{phen})_3]^{2+}$, which occurs by outer-sphere electron transfer, the rates are increased by the addition of pyridine, which assists in the deprotonation of ArCH_3^+ .^{11a}

Correlation between Rate Constants and Redox Potentials. For an outer-sphere electron transfer mechanism, rate constants should correlate with redox potentials according to Marcus theory:²²

$$k_{12} = (k_{11}k_{22}K_{12}f_{12})^{1/2} \quad (10)$$

$$\log f_{12} = \frac{(\log K_{12})^2}{4 \log(k_{11}k_{22}/Z^2)} \quad (11)$$

Figure 5 shows a plot of $\log k_2$ versus $\Delta E^0 \{ \Delta E^0 = E^0(\text{Ru}^{\text{VI}}/\text{Ru}^{\text{V}} - E^0(\text{ArCH}_3^+/\text{ArCH}_3)) = 0.94 \text{ V} - E^0(\text{ArCH}_3^+/\text{ArCH}_3) \}$, for those alkylaromatic compounds where accurate E^0 values are available.²³ A roughly linear correlation is found; however, the slope is rather small (2.8 ± 0.5), indicating that there is very little charge transfer from the substrates to Ru^{VI} in the transition state. According to the Marcus theory, for highly endergonic outer-sphere electron transfer reactions, the slope should be around 17 V^{-1} .²⁴ The dotted line in Figure 5 shows the theoretical curve for $\log k_2$ vs ΔE^0 for outer-sphere electron transfer. This line is constructed according to eq 10 (neglecting work terms) using a self-exchange rate of $1 \times 10^5 \text{ M}^{-1} \text{ s}^{-1}$ for the $[\text{Ru}^{\text{VI}}(\text{L})(\text{O})_2]^{2+}/[\text{Ru}^{\text{V}}(\text{L})(\text{O})_2]^+$ couple and a self-exchange rate of $1 \times 10^3 \text{ M}^{-1} \text{ s}^{-1}$ for the $\text{ArCH}_3^+/\text{ArCH}_3$ couples.²⁵ The

(22) Marcus, R. A.; Eyring, H. *Annu. Rev. Phys. Chem.* **1964**, *15*, 155–196.

(23) Howell, J. O.; Goncalves, J. M.; Amatore, C.; Klasinc, L.; Wightman, R. M.; Kochi, J. K. *J. Am. Chem. Soc.* **1984**, *106*, 3968–3976.

(24) Andrieux, C. P.; Blocman, C.; Dumas-Bouchiat, J.-M.; Saveant, J.-M. *J. Am. Chem. Soc.* **1979**, *101*, 3431–3441.

(25) Reed, R. A.; Murray, R. W. *J. Phys. Chem.* **1986**, *90*, 3829–3835.

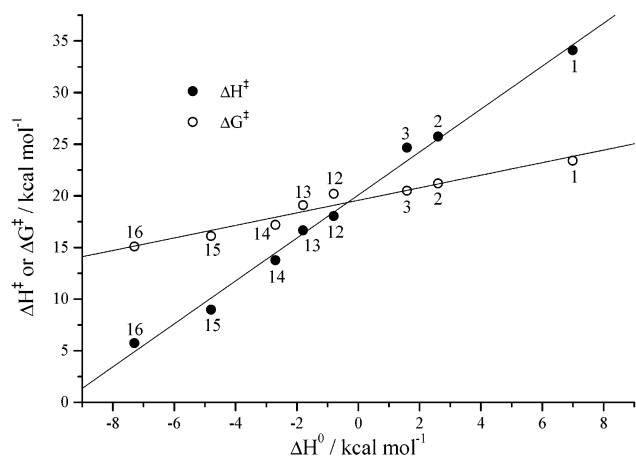


Figure 6. Plot of ΔH^\ddagger and ΔG^\ddagger versus ΔH^0 for the hydrogen atom transfer step in the oxidation of alkylaromatic compounds by $[\text{Ru}^{\text{VI}}(\text{L})(\text{O})_2]^{2+}$ in CH_3CN at 298 K (for ΔG^\ddagger plot, slope = 0.61 ± 0.06 , $r = 0.975$; for ΔH^\ddagger plot, slope = 2.1 ± 0.1 , $r = 0.996$).

theoretical curve has a much larger slope (ca. 17 V^{-1}) and is far below the experimental curve, clearly indicating that an outer-sphere electron transfer mechanism is not operating.²⁶

Correlation between Rate Constants and α C–H Bond Strength of Alkylaromatic Compounds. If the reactions occur by a hydrogen atom transfer pathway, then the rates should correlate with the C–H bond strengths of the substrates.^{2,3} Figure 6 shows plots of ΔH^\ddagger and ΔG^\ddagger vs ΔH^0 . ΔH^0 is the difference between the strength of the bond being broken and that being formed in a H-atom transfer step (eq 7), i.e., $\Delta H^0 = \text{BDE of ArCH}_2\text{–H} - \text{BDE of } [\text{O}=\text{Ru}^{\text{V}}(\text{L})\text{O–H}]^{2+}$. BDE of $[\text{O}=\text{Ru}^{\text{V}}(\text{L})\text{O–H}]^{2+}$ has been calculated to be $82.8 \text{ kcal mol}^{-1}$.⁹ BDE of $\text{ArCH}_2\text{–H}$ is available only for some of the substrates, and they are listed in Table 1. A good linear correlation between ΔG^\ddagger and ΔH^0 is found, which strongly supports a hydrogen atom transfer mechanism for the oxidation of these substrates by $\text{trans-}[\text{Ru}^{\text{VI}}(\text{L})(\text{O})_2]^{2+}$. ΔH^\ddagger also correlates with ΔH^0 since ΔH^\ddagger is proportional to ΔS^\ddagger . Similar correlations have been observed in the oxidation of alkylaromatic hydrocarbons by CrO_2Cl_2 ³ and ${}^{\text{n}}\text{Bu}_4\text{N-}[\text{MnO}_4]^{2-}$ ^{2b} and in the oxidation of phenols by $\text{trans-}[\text{Ru}^{\text{VI}}(\text{L})(\text{O})_2]^{2+}$.⁹ Recently, a variety of H-atom transfer reactions have been shown to follow the Marcus cross relation.²⁷ In the context of Marcus theory, the observation of a linear correlation between ΔG^\ddagger and ΔH^0 in this case means that the H-atom self-exchange rates of the alkylaromatics are similar. The slope of (0.61 ± 0.06) in the $\Delta G^\ddagger/\Delta H^0$ plot is in reasonable agreement with the theoretical slope of 0.5 predicted by the Marcus theory (for $\Delta G^0 \approx 0$ and assuming $\Delta H^0 \approx \Delta G^0$). The rate constants for H-atom abstraction from various alkylaromatic compounds by $\text{trans-}[\text{Ru}^{\text{VI}}(\text{L})(\text{O})_2]^{2+}$ also correlate with the rates of abstraction by ${}^t\text{BuOO}\cdot$, ${}^t\text{BuO}\cdot$, and MnO_4^- ; plots of $\log k_2'$ vs the strength of the O–H bond formed by the oxidants are roughly linear (Figure 7).

(26) It is assumed that deprotonation of ArCH_3^+ is rapid (eq 5). If deprotonation is rate-limiting then the theoretical rate constants would be even smaller.

(27) Roth, J. P.; Yodar, J. C.; Won, T.-J.; Mayer, J. M. *Science* **2001**, *294*, 2524–2526.

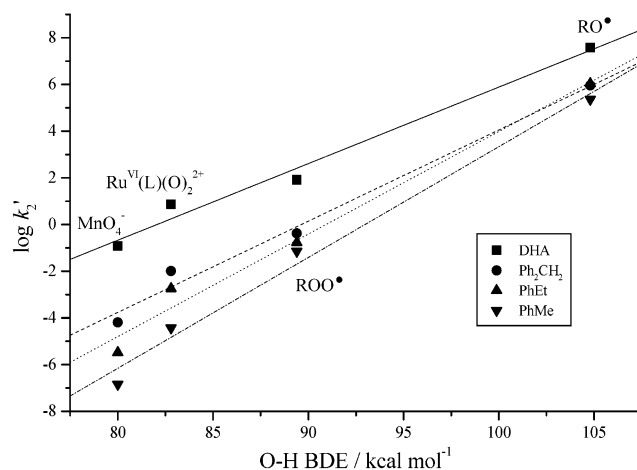


Figure 7. Plot of $\log k_2'$ (the rate constant for H-atom abstraction, per H-atom) versus the strength of the O–H bond formed by the oxidants. Solid line (DHA), slope = 0.33 ± 0.03 , $r = 0.991$. Dash line (Ph_2CH_2), slope = 0.39 ± 0.03 , $r = 0.994$. Dot line (PhEt), slope = 0.44 ± 0.04 , $r = 0.992$. Dash-dot line (PhMe), slope = 0.47 ± 0.04 , $r = 0.994$.

Such a correlation is typical of H-atom transfer reactions.²⁸ A similar correlation is also found in the oxidation of phenols by $\text{trans-}[\text{Ru}^{\text{VI}}(\text{L})(\text{O})_2]^{2+}$ and various oxygen radicals.⁹

H-Atom Self-Exchange Rates of $[\text{Ru}^{\text{VI}}(\text{L})(\text{O})_2]^{2+}$. Using the Marcus cross relation (eq 10), we were able to estimate the $[\text{Ru}^{\text{VI}}(\text{L})(\text{O})_2]^{2+}/[\text{Ru}^{\text{V}}(\text{L})(\text{O})(\text{OH})]^{2+}$ self-exchange rate. The self-exchange rate for $\text{PhCH}_3/\text{PhCH}_2\cdot$ is reported to be $\sim 4 \times 10^{-5} \text{ M}^{-1} \text{ s}^{-1}$ at 298 K.²⁷ ΔG^0 for the reaction between Ru^{VI} and PhCH_3 is evaluated using the equation: $\Delta G^0 = \Delta H^0 = \text{BDE of PhCH}_2\text{–H} - \text{BDE of } [\text{O}=\text{Ru}^{\text{V}}(\text{L})\text{O–H}]^{2+} = (89.8 - 82.8) = 7 \text{ kcal mol}^{-1}$. The rate constant for the cross reaction is $1.11 \times 10^{-4} \text{ M}^{-1} \text{ s}^{-1}$ at 298 K. Using these data, we estimated the $[\text{Ru}^{\text{VI}}(\text{L})(\text{O})_2]^{2+}/[\text{Ru}^{\text{V}}(\text{L})(\text{O})(\text{OH})]^{2+}$ self-exchange rate to be $2 \times 10^1 \text{ M}^{-1} \text{ s}^{-1}$ at 298 K.

Conclusions

The oxidation of a series of 21 alkylaromatic compounds in CH_3CN by $\text{trans-}[\text{Ru}^{\text{VI}}(\text{L})(\text{O})_2]^{2+}$ occurs by initial, rate-limiting hydrogen atom transfer. The resulting organic radicals are trapped by rapid $\text{HO}\cdot$ transfer from $\text{trans-}[\text{Ru}^{\text{V}}(\text{L})(\text{O})(\text{OH})]^{2+}$ to give the corresponding alcohol products. This process occurs rapidly in the solvent cage since added BrCCl_3 and O_2 have no effects on the reaction rates. In the oxidation of DHA, the formation of anthracene probably arises from a second H-atom transfer from the hydroanthracenyl radical to $\text{trans-}[\text{Ru}^{\text{VI}}(\text{L})(\text{O})_2]^{2+}$.^{29,30} Primary and secondary alcohol products are further rapidly oxidized to the corresponding carbonyl products. A linear correlation of ΔH^\ddagger and ΔS^\ddagger is found, which supports a common mechanism for all the substrates. ΔH^\ddagger and ΔG^\ddagger correlate with ΔH^0 for the hydrogen transfer step according

(28) (a) *Free Radicals*; Kochi, J. K., Ed.; Wiley: New York, 1973; Vol. 1, pp 275–331. (b) Korček, S.; Chenier, J. H. B.; Howard, J. A.; Ingold, K. U. *Can. J. Chem.* **1972**, *50*, 2285–2297. (c) Tedder, J. M. *Angew. Chem., Int. Ed. Engl.* **1982**, *21*, 401–410.

(29) The detailed mechanism for the oxidation of DHA will be further investigated.

(30) A report on the oxidation of DHA and other substrates by $[(\text{bpy})_2\text{(py)Ru}^{\text{IV}}\text{O}]^{2+}$ has just appeared: Bryant, J. R.; Mayer, J. M. *J. Am. Chem. Soc.* **2003**, *125*, 10351–10361.

to the Marcus equation. Hydrogen atom transfer occurs instead of electron transfer for these reactions because of a more favorable ΔG^0 . According to the Marcus cross relation, the rate of a chemical reaction depends on both the self-exchange rates of the reactants and ΔG^0 of the reaction. The H-atom self-exchange rates of $\text{Ru}^{\text{VI}}/\text{Ru}^{\text{V}}$ ($2 \times 10^1 \text{ M}^{-1} \text{ s}^{-1}$) and $\text{ArCH}_3/\text{ArCH}_2^\bullet$ ($\sim 4 \times 10^{-5} \text{ M}^{-1} \text{ s}^{-1}$) are both slower than their corresponding electron self-exchange rates ($1 \times 10^5 \text{ M}^{-1} \text{ s}^{-1}$ and $\sim 1 \times 10^3 \text{ M}^{-1} \text{ s}^{-1}$). However, in the oxidation of toluene, one of the least reactive substrates, the H-atom transfer process is uphill by only 7 kcal mol⁻¹ while the electron transfer process is uphill by 39 kcal mol⁻¹. In the oxidation of DHA, one of the most reactive substrates, the H-atom transfer process is downhill by ~ 5 kcal mol⁻¹, but the electron transfer process is uphill by ~ 13 kcal mol⁻¹.

The oxidation of a series of phenols by *trans*- $[\text{Ru}^{\text{VI}}(\text{L})(\text{O})_2]^{2+}$ has also been shown to occur via a H-atom transfer mechanism.⁹ The PhO–H bond strength (90 kcal mol⁻¹) is the same as that of toluene,³¹ yet phenol is 2×10^4 times more reactive than toluene. A logical explanation is that phenol has a faster H-atom self-exchange rate. If we take

(31) Blanksby, S. J.; Ellison, G. B. *Acc. Chem. Res.* **2003**, *36*, 255–263.

the $[\text{Ru}^{\text{VI}}(\text{L})(\text{O})_2]^{2+}/[\text{Ru}^{\text{V}}(\text{L})(\text{O})(\text{OH})]^{2+}$ self-exchange rate to be $2 \times 10^1 \text{ M}^{-1} \text{ s}^{-1}$ at 298 K, then the PhOH/PhO[•] self-exchange rate is estimated to be $\sim 5 \times 10^4 \text{ M}^{-1} \text{ s}^{-1}$ at 298 K, about 9 orders of magnitude faster than that of $\text{ArCH}_3/\text{ArCH}_2^\bullet$.

Acknowledgment. The work described in this paper was supported by the Research Grants Council of Hong Kong (CityU 1097/98P) and the Area of Excellence Scheme (AoE/P-10-01) established under the University Grants Council (HKSAR) and the University Development Fund of the University of Hong Kong.

Supporting Information Available: Table of rate data and representative kinetic plots. This material is available free of charge via the Internet at <http://pubs.acs.org>.

IC034782J

(32) (a) Parker, V. D. *J. Am. Chem. Soc.* **1992**, *114*, 7458–7462. (b) Bordwell, F. G.; Cheng, J. P.; Ji, G. Z.; Satish, A. V.; Zhang, X. *J. Am. Chem. Soc.* **1991**, *113*, 9790–9795. (c) *CRC Handbook of Chemistry and Physics*, 82nd ed.; Lide, D. R. Ed.; CRC Press: Boca Raton, 2001.